11th International Symposium on Turbulence and Shear Flow Phenomena (TSFP11)
Southampton, UK, July 30 to August 2, 2019

EXPERIMENTAL INVESTIGATION ON THE INFLUENCE OF INCOMING AND LOCAL STRATIFICATION ON FLOW AND DISPERSION IN IDEALIZED URBAN GEOMETRIES

Davide Marucci
EnFlo, Department of Mechanical Engineering Sciences
University of Surrey
Guildford, GU2 7XH, UK
d.marucci@surrey.ac.uk

Matteo Carpentieri
EnFlo, Department of Mechanical Engineering Sciences
University of Surrey
Guildford, GU2 7XH, UK
m.carpentieri@surrey.ac.uk

ABSTRACT

In urban environments at neighbourhood and microscales, stratification effects are clearly significant both on processes at the top of the boundary layer and in the outer suburbs and semi-rural areas surrounding dense cities (Hunt *et al.*, 2004). This work aims to investigate this aspect by means of wind tunnel experiments. Both stable and unstable stratification have been considered and flow and pollutant concentration measurements were performed on an array of cuboids. Clear stratification effects on the plume shape and turbulence in and above the canopy were captured and described. Then the focus moved to local stratification, obtained by either heating or cooling the building walls of a bi-dimensional street canyon, also in combination with a stably-stratified incoming boundary layer. This represents an absolute novelty and the results highlight how both local and incoming stratification can significantly affect the flow and dispersion at a microscale level in a complex way that depends on the particular case of study.

INTRODUCTION

When simulating urban dispersion, the large surface roughness is often ascribed as an argument to avoid the complication of considering thermal effects, by noting that any stratification would be weakened to the point of being irrelevant. Nevertheless, strictly speaking neutral boundary layers (NBL) are way less frequent than convective (CBL) and even stable (SBL) over cities (see e.g. field observations from Wood *et al.* 2010). For this reason, we believe that an investigation of the effects of atmospheric stratification on flow and dispersion in urban areas is of great interest, also considering the scarcity of detailed experimental studies on the topic.

Only few wind tunnel studies have been attempted to date, mainly focussing on the effects of buoyancy forces. Among them, Uehara *et al.* (2000) simulated an array of aligned cubic blocks with stratified (stable and convective) approaching flow. Kanda & Yamao (2016), instead, considered a staggered array of cubic blocks. On the other hand, Kovar-Panskus *et al.* (2002) and Allegrini *et al.* (2013) focussed on local stratification, investigating the case of differential heating for a bi-dimensional street cavity.

The research focussed initially on the generation of the approaching flow to the model. For this purpose, artificially thickened SBL, NBL and CBL were simulated in the EnFlo meteorological wind tunnel over a very rough surface (as detailed by Marucci *et al.* 2018). Then, these BLs were firstly applied to an array of rectangular blocks and then to an isolated bi-dimensional street canyon. In the latter the effect of local differential heating was also taken into account by heating or cooling the walls and/or ground.

METHODS

The EnFlo open-return meteorological wind tunnel has a working section 20 m long, 3.5 m wide and 1.5 m high. A series of 15 horizontal heaters upstream of the working-section allows a vertical temperature profile to be imposed at the inlet, while the floor can be cooled or heated as needed. As boundary-layer artificial-thickening devices, triangular spires were employed coupled with rectangular roughness elements on the floor. Appropriate inlet temperature profiles were then imposed (see Marucci *et al.* 2018), resulting in BLs ranging in height from 0.85 to 1.30 m.

Velocity measurements were carried out by means of two-component laser-Doppler anemometry (LDA). Mean and fluctuating temperature and concentration measurements were made using a cold-wire probe (CW) and a fast flame ionisation detector (FFID), held close to the LDA measuring volume (about 4 to 5 mm downstream) so as to allow measurement of the turbulent heat and concentration fluxes. A reference wind tunnel velocity U_{REF} was sampled with a sonic anemometer placed at a height of 1 m, 5 m from the test section inlet.

Two model geometries were considered. The first one

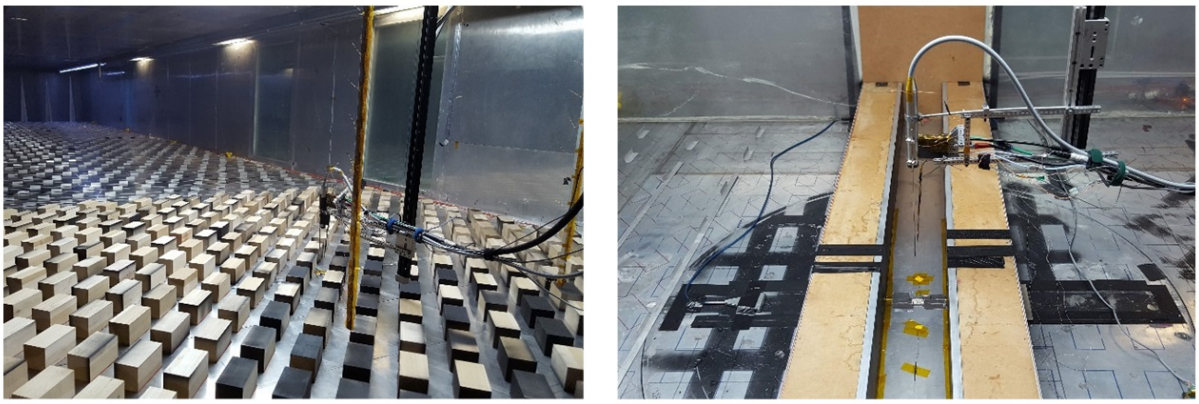

Figure 1. Array of rectangular blocks (on the left) and bi-dimensional street canyon (on the right).

is an array of 24x14 rectangular wooden blocks with dimensions $H \times 2H \times H$ and spaced H, where H is equal to 70 mm. Measurements were performed at 0 and 45° wind directions. Propane was released at ground level from a circular source as a passive tracer conveniently mixed with air. The second geometry studied was an isolated bi-dimensional street canyon, with aspect ratio 1, width to height ratio of 15, model height 166 mm. The square cross-section buildings were designed in order to have one wall heated with heater mats and the opposite cooled by means of circulating water. Five different heating/cooling configurations were investigated: no local heating, windward wall, leeward wall, ground or all three surfaces heated. The experiments were repeated with neutral and stable approaching flow. Propane was released at ground level from the centre of the street canyon. More details can be found in Marucci & Carpentieri (2019). Pictures of the two models are displayed in Figure 1.

RESULTS

Array of Buildings: Influence of Incoming Stratification

The level of stability of the approaching flow is here labelled with the bulk Richardson number, estimated as $Ri_\delta^{app} = g(\overline{\Theta}_\delta - \Theta_0)\delta/(\Theta_0 \overline{U}_\delta^2)$, where g is the gravity acceleration, δ the boundary layer depth, Θ_0 is the temperature at z = 2 mm (approximately equivalent to the aerodynamic roughness length). Six stratification levels were considered, corresponding to Ri_δ^{app} 0.29, 0.21, 0.14, 0, -0.5 and -1.5. The reference neutral case was repeated with the SBL and CBL setup. For all the cases, a horizontal scan of the plume was performed at two heights inside and above the canopy (z/H = 0.5 and 1.5, respectively), as well as vertical scans along the centreline of the plume.

Table 1 summarises some important parameters. The friction velocity (u_*), aerodynamic roughness length (z_0) and displacement height (d) are measured, as described in Marucci *et al.* (2018), from a fitting of the roughness sublayer region over the array, found here to happen in the range $z/H = 2 \div 4$. All of these quantities show a dependency from the stratification. Finally also a Richardson number Ri_H measured over the array is shown, in which the reference height and velocity are the building height and the averaged velocity measured at this height, while the temperature difference is the difference between the averaged values measured at roof height and a reference sampled at 10 mm in the canopy.

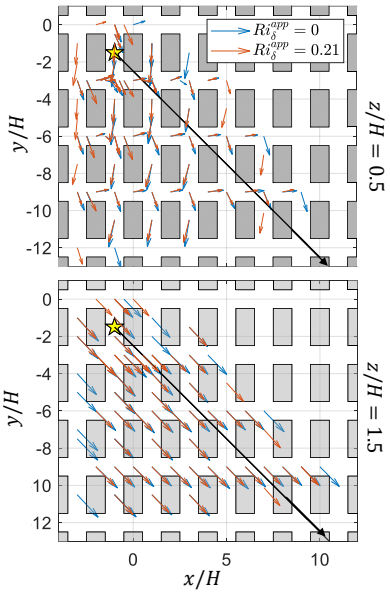

Figure 2. Planar view of mean horizontal velocity vectors inside and above the canopy for SBL and NBL and wind 45°. Black arrow is free-stream wind direction while the yellow star is the location of the pollutant source.

Figure 2 shows the vectors of horizontal velocity for a neutral and stable case. No effects on the channelling inside the streets are experienced by the flow, while the module of the velocity appears generally reduced by stratification. At a height of $1.5H$ the flow is already aligned with the free stream, both in the NBL and in SBL case. In Figure 3 the horizontal contour plots of the non-dimensional mean concentration inside the canopy for SBL, NBL and CBL are presented. At $z/H = 0.5$ inside the canopy the axis of the plume is not affected by the stable stratification (being deviated of about 15° for both SBL and NBL). Differently, in the CBL such angle is increased to 18°). Above the canopy at $z/H = 1.5$ both the non-neutral stratification cases show an increment of about 2° in the angle respect to the neutral case. The concentrations appear increased by the application of the stable stratification and reduced by the convective one, effects which become more and more evident farther from the source.

Figure 4 also shows vertical profiles of mean concentration at the centre of an intersection $6H$ far from the

Table 1. Urban array cases parameters at wind direction 45°.

	CBL			SBL			
Ri_δ^{app}	**-1.5**	**-0.5**	**0**	**0**	**0.14**	**0.21**	**0.29**
U_{REF} (m/s)	1.0	1.25	1.25	1.25	1.25	1.25	1.15
u_*/U_{REF}	0.118	0.105	0.081	0.078	0.063	0.061	0.059
z_0 (mm)	6.2	6.3	4.0	3.4	2.5	2.6	2.9
d (mm)	21	23	51	52	53	54	55
Ri_H	-0.19	-0.15	0	0	0.10	0.19	0.28

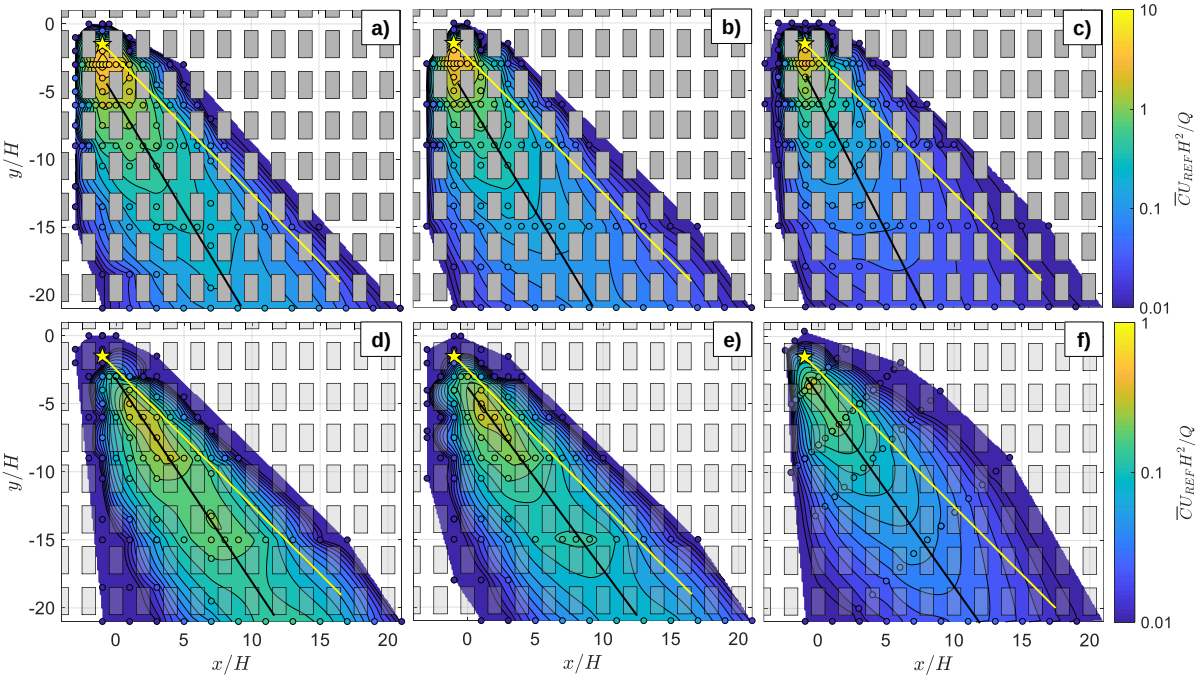

Figure 3. Contour graphs of non-dimensional mean concentration for different level of stability at $z/H = 0.5$ (a-c) and $z/H = 1.5$ (d-f). $Ri_\delta^{app} = 0.21$ (a,d), $Ri_\delta^{app} = 0$ (b,e), $Ri_\delta^{app} = -1.5$ (c,f). Yellow line is free-stream wind direction, yellow star is the ground source location, black line is the estimated plume axis. For brevity only the reference neutral case measured with the SBL setup is shown in (b,e). Q is the pollutant tracer flow rate from the source.

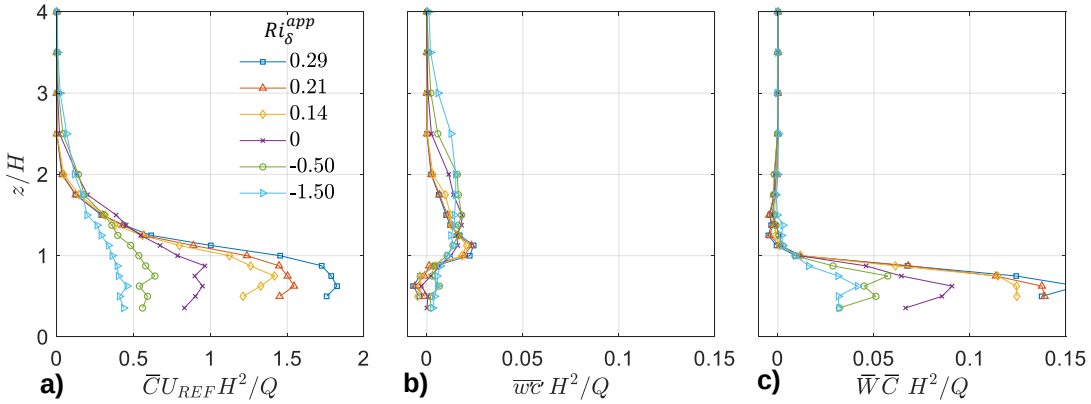

Figure 4. Vertical profiles of non-dimensional mean concentration (a), turbulent (b) and mean (c) vertical pollutant fluxes for different level of stability at the centre of an intersection ($x/H = 1$, $y/H = -6$). For brevity only the reference neutral case measured with the CBL setup is shown.

source. The concentrations within the canopy are doubled for the strongest SBL, compared to the reference NBL, and one half for the CBL. The plume height is affected as well, with a reduction of 20% for the SBL (independently from the intensity) and an increment of the same amount for the CBL. Such profiles were fitted with a Gaussian curve to find the σ_z coefficient representative of the plume height. The same was done for the lateral profiles perpendicular to the plume axis (extrapolated from the contour graphs of Figure 3) to find σ_h, representative of the plume width. Very small stratification effects were found on σ_h, compared to the effects experienced by σ_z, which was up to 40% lower in the most stable case and up to 150% larger in the most unstable, compared to the reference neutral. This is in agreement with what observed by Briggs (1973) in field experiments over urban roughness. On the contrary, Kanda & Yamao (2016) found an opposite behaviour, with the plume height almost unaffected and the width sensibly reduced by the application of stable stratification. They were not able to explain such a peculiar behaviour.

In Figure 4 also the vertical fluxes at the centre of an intersection are shown. Inside the canopy the fluxes are strongly dependent on the location, hence a generalization is difficult. Nevertheless, it can be noted that at least at the centre of the intersection the turbulent component is negligible, while at the roof level it becomes roughly equivalent to the mean flux for all the stratification conditions. Above the canopy the turbulent flux is then predominant. The latter appears to scale with the vertical mean concentration gradient in all the stability cases investigated, as already found for the NBL by Carpentieri *et al.* (2012).

2D Street Canyon: Influence of Incoming and Local Stratification

The experiments on the bi-dimensional street canyon focused on the central cross-section, with measurements up to $2H$. The investigated free-stream velocities ranged from 1.25 down to 0.5 m/s. Most of the dataset was acquired at 0.65 m/s, considered a good compromise between the necessity of Reynolds number independence and local stratification intensity. The latter was estimated by means of the local Richardson number, calculated as $Ri_{Local} = g\left(\Theta_{2H} - \Theta_{HOT}\right)H/\left(\Theta_{2H}U_{2H}^2\right)$ where Θ_{HOT} is the temperature of the heated surfaces and Θ_{REF} the temperature at $z/H = 2$. Ri_{Local} up to -2.0 were simulated, while the stable approaching flow was, for most of the cases, equivalent to $Ri_{\delta}^{app} = 0.39$. For brevity, here only six cases will be presented: no heating (NH), windward wall heated (WH), leeward wall heated (LH), all with neutral and stable approaching flow (in the latter the cases are called SNH, SWH and SLH, respectively). Ri_{Local} is about -1.2 in all the presented wall-heated cases.

Figure 5 shows the contours of mean velocity and velocity streamlines, as well as vertical profiles for $x/H = 0$ and longitudinal profiles at $z/H = 0.5$. The flow structure inside the canyon in the NH case is characterised by a single-vortex pattern with centre located along the vertical canyon centreline at about $z/H = 0.6$. The same overall structure is found for the LH case as well. Differently, in the WH case a second counter-rotating vortex appears, generated by the buoyancy forces produced by the heated wall, which opposes the descending motion of the air into the canyon and slows down the velocity (as also found by e.g. Allegrini *et al.*, 2013 and Cai, 2012). The application of the SBL in the present study has the effect of a reduction in the mean velocity, mainly in the bottom half of the canyon (as also shown by e.g. Li *et al.*, 2016). The SWH case, in particular, experiences a larger slowing down of the speed, bringing to the formation of almost-zero velocity regions within the canopy. Differently, in the SLH case the SBL exerts a much lower reduction on the mean velocity field. In fact, since local heating and stable approaching flow have opposite effects on the mean velocity field, in this particular case the local heating overcomes the incoming stability.

The profiles of measured averaged turbulent kinetic energy $TKE = 3/4\left(\overline{u'^2} + \overline{w'^2}\right)$ are shown in Figure 6a and d. In all cases the largest values are found between $z = H$ and $1.5H$. In the WH case, an increasingly turbulent region appears close to the heated wall. Allegrini *et al.* (2013) found the maximum TKE values in the same area, and this was attributed to the cold air entering the canyon and hitting the warmer air, which is rising due to buoyancy at the windward wall. Moreover, the longitudinally-averaged profile grows almost linearly in the canopy. In the LH case, differently, the increase of TKE in the canyon is smaller and not located near the heated wall, but closer to the windward wall again. The stable stratification generates a very strong and generalised reduction of TKE both above and inside the canopy, also in the presence of wall heating. This is estimated in an average reduction inside the canopy of 50, 46 and 30%, respectively for the SNH, SWH and SLH cases, compared to the NBL cases.

Also profiles of averaged concentration derived from releasing a passive tracer from a ground point source are shown in Figure 6b and e. The NH case is characterised by a large concentration region upstream the source rising along the leeward wall up to the street canyon top, where some pollutant is re-entrained inside the canopy while other is carried downstream by the mean flow. In the WH case the pollutant transport by means of the main vortex is weakened by the action of the buoyancy force. Moreover, concentration values are increased downstream the source closer to the ground and along the windward wall, the latter due to pollutant up-drafts. For the LH case no significant differences are found in the cross-section compared to the NH case, despite the strengthened main vortex. The application of the incoming SBL creates a generalised increase of concentration inside the canopy. For SNH the averaged concentration in the canopy is increased by about 75% compared to the NH case. Such increment is very close to what found by Li *et al.* (2016) for a line source with a similar level of stratification. An even larger increment of concentration is experienced by the SWH case, which has a level of pollutant within the canopy that is double compared to the NBL counterpart. Such strong increase is concentrated mostly in the lower half of the canopy, thus more significant at pedestrian level. The increment for the SLH case is more modest, with a 55% increase. Looking at the longitudinal profiles of vertically-averaged concentration, it is possible to observe how, while for the NH and LH case the high level of pollutant close to the leeward wall is even increased by the SBL, for the WH and SWH it is consistently lower. In the latter, the region of larger concentration is moved towards the centre of the canyon, driven by the velocity stagnation region which determines a large level of concentration immediately after the source release.

Two quantities have also been computed to evaluate the pollutant removal from the canopy: the pollutant exchange rate (PCH) and the air exchange rate (ACH). They have been computed as $\overline{PCH} = \int_W \overline{w(t)c(t)}dx$ and $\overline{ACH} =$

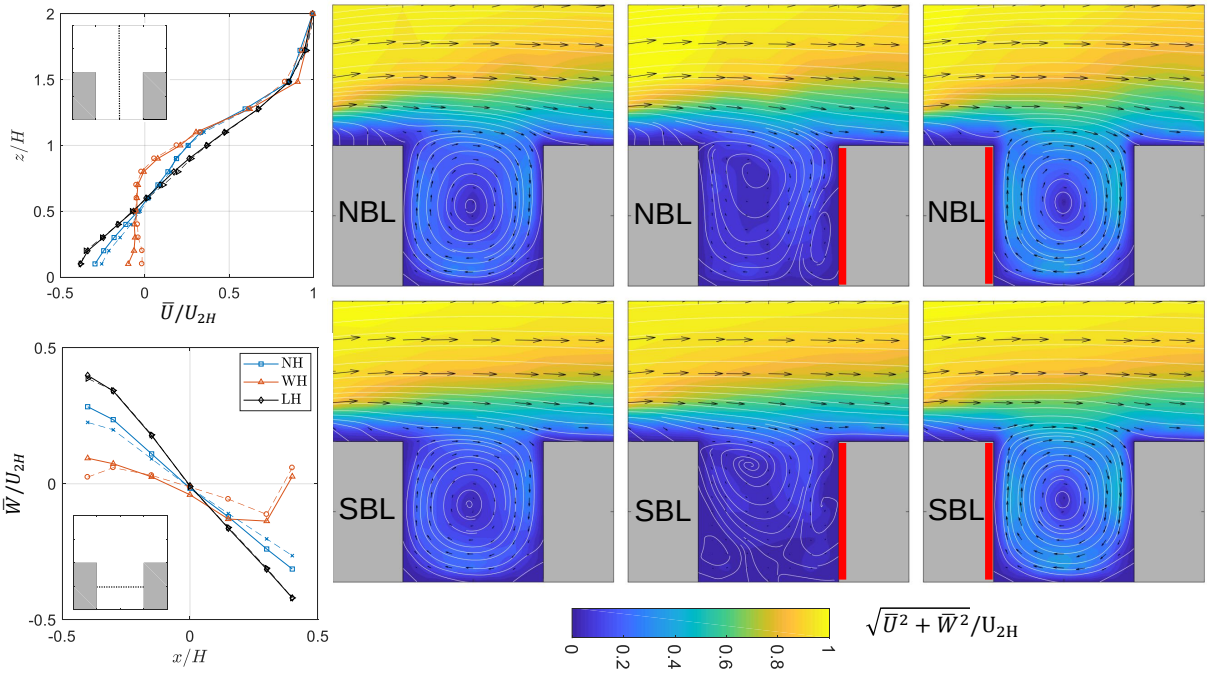

Figure 5. Contours and vectors of mean velocity, white lines are streamlines. The red lines represent the heated surfaces in each case ([S]NH left, [S]WH centre, [S]LH right). The line plots on the left represent the vertical profiles of mean streamwise velocity at $x/H = 0$ (top) and the longitudinal profiles of mean vertical velocity at $z/H = 0.5$ (bottom); NBL = continuous lines, SBL = dashed lines.

$\int_W \overline{w(t)}dx$ (with W canyon width), assuming that the measuring time is long enough to get statistically representative samples. The two rates have then been decomposed in $\overline{PCH^+}$, $\overline{ACH^+}$ and $\overline{PCH^-}$, $\overline{ACH^-}$ considering, respectively, only either positive or negative instantaneous velocity samples, while the others are alternatively imposed equal to zero (the positive rates representing the removal of pollutant/air from the street canyon, the negative ones the pollutant/air re-entrainment into the cavity). To get a better insight of the vertical ventilation, the exchange rates are computed at different heights in the canyon, as displayed in Figure 6c and f.

In the NH case, $\overline{ACH^+}$ shows a maximum approximately at the height of the main vortex centre (as also found by Garau *et al.*, 2018) followed by a decrease up to the canyon top. The LH case shows a similar trend, but with amplified values due to the larger velocity magnitudes. On the other hand, in the WH case $\overline{ACH^+}$ almost monotonically increases with height, but with lower values compared to the other case. The application of SBL has the general effect of decreasing the exchange rate, following the reduction in the mean and fluctuating velocities previously discussed. The observed decrease in the exchange rate is rather limited for the LH case, for which the stable stratification had only a small impact on the mean flow.

$\overline{PCH^+}$ presents a different trend, namely a reduction with height thanks to the larger values of concentration in the bottom region. Despite this, the three local heating configurations are still organised with WH, NH and LH in growing order of exchange rate values. In this case, the effect of stable stratification is interestingly seen to produce opposite effects compared to $\overline{ACH^+}$. On average $\overline{PCH^+}$ is increasing within the canopy, especially for SLH, while the air exchange rate did not show a significant modification in that case. On the other hand, the SWH case does not show significant variations from WH. This discrepancy might be up to the fact that concentrations in SBL were found to increase more than the velocity reduction, hence resulting in an increase of $\overline{PCH^+}$ values. Finally, $\overline{PCH^+}$ at roof level are found to be approximately twice as large as $\overline{PCH^-}$, confirming the results by Liu *et al.* (2005), despite the different type of source.

CONCLUSION

Two extensive wind tunnel experimental campaigns were conducted in order to investigate the effect of thermal stratification on flow and dispersion in complex geometries. From the regular array of rectangular building case with wind direction 45° it can be concluded that in both SBLs and CBLs the plume width and axis are only slightly modified by the applied stratification. Differently, the plume height as well as the mean concentration values are clearly affected in a specular way. In SBL the vertical displacement is reduced, and the pollutant is trapped close to the canopy more than doubling the concentration level and reducing the plume height. In CBL, instead, the opposite behaviour was found, with lower concentration (up to three times respect to NBL) and taller plumes.

In the bi-dimensional street-canyon case the combined effect of incoming and local stratification was investigated. The largest changes on the flow structure were found for the case with windward wall heated, with a second counter-rotating vortex appearing close to the heated wall. The concentrations are increased in all the cases considering the SBL as approaching flow, with the maximum increments at pedestrian level in case of windward heated wall.

The produced dataset represents valuable validation cases for models and CFD simulations.

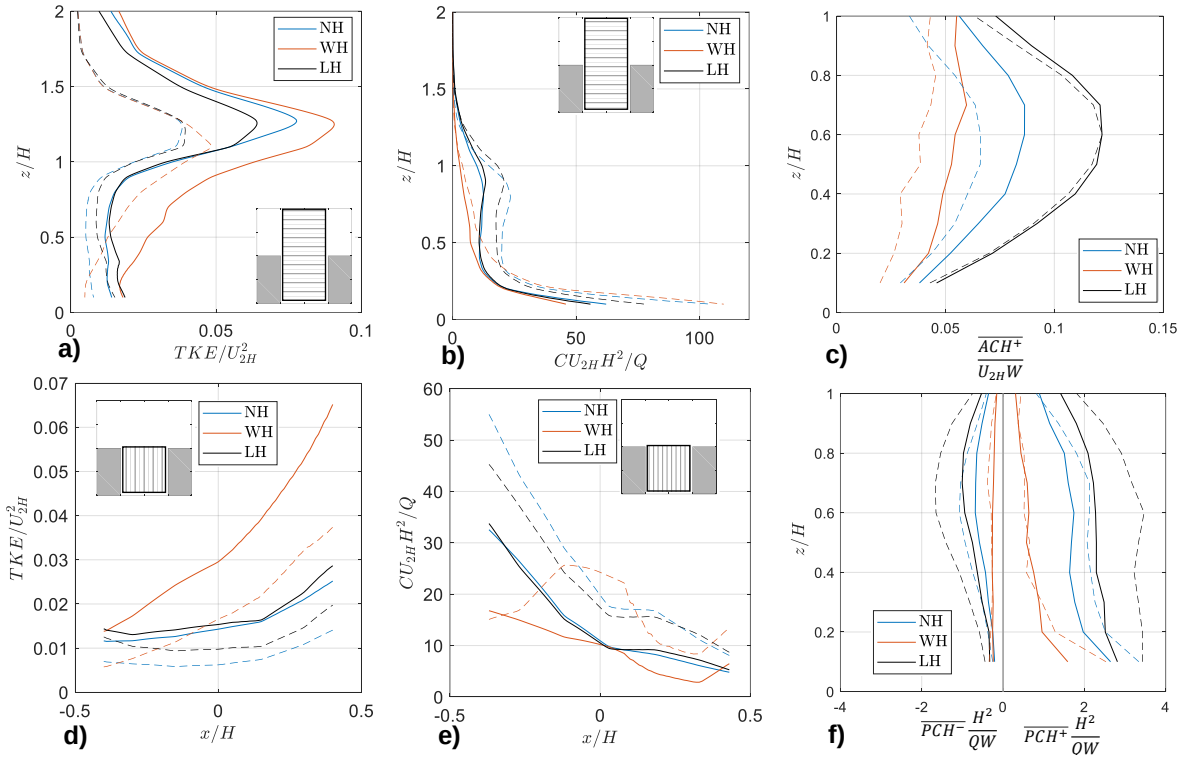

Figure 6. Vertical profiles of longitudinally-averaged TKE and mean concentration (a-b) and longitudinal profiles of vertically-averaged TKE and mean concentration (d-e); vertical profiles of $\overline{ACH^+}$, $\overline{PCH^+}$ and $\overline{PCH^-}$ (c-f). NBL = continuous lines, SBL = dashed lines.

REFERENCES

Allegrini, Jonas, Dorer, Viktor & Carmeliet, Jan 2013 Wind tunnel measurements of buoyant flows in street canyons. *Building and Environment* **59**, 315–326.

Briggs, Gary A. 1973 Diffusion Estimation for Small Emissions. *Tech. Rep.*. Atmospheric Turbulence and Diffusion Laboratory. NOAA/ATDL ATDL-106.

Cai, Xiaoming 2012 Effects of Wall Heating on Flow Characteristics in a Street Canyon. *Boundary-Layer Meteorology* **142** (3), 443–467.

Carpentieri, Matteo, Hayden, Paul & Robins, Alan G. 2012 Wind tunnel measurements of pollutant turbulent fluxes in urban intersections. *Atmospheric Environment* **46**, 669–674.

Garau, Michela, Badas, Maria Grazia, Ferrari, Simone, Seoni, Alessandro & Querzoli, Giorgio 2018 Turbulence and Air Exchange in a Two-Dimensional Urban Street Canyon Between Gable Roof Buildings. *Boundary-Layer Meteorology* **167** (1), 123–143.

Hunt, J.C.R., Britter, R.E., Carruthers, D.J. & Daish, N.C. 2004 Dispersion from Accidental Releases in Urban Areas UK Atmospheric Dispersion Modelling. *Tech. Rep.*. Liaison Committee Report No. ADMLC/2002/3.

Kanda, Isao & Yamao, Yukio 2016 Passive scalar diffusion in and above urban-like roughness under weakly stable and unstable thermal stratification conditions. *Journal of Wind Engineering and Industrial Aerodynamics* **148**, 18–33.

Kovar-Panskus, A, Moulinneuf, L, Savory, E, Abdelqari, A, Sini, J F, Rosant, J M, Robins, A & Toy, N 2002 A wind tunnel investigation of the influence of solar-induced wall-heating on the flow regime within a simulated urban street canyon. *Water, Air, & Soil Pollution: Focus* **2** (5-6), 555–571.

Li, Xian Xiang, Britter, Rex & Norford, Leslie K. 2016 Effect of stable stratification on dispersion within urban street canyons: A large-eddy simulation. *Atmospheric Environment* **144**, 47–59.

Liu, Chun Ho, Leung, Dennis Y C & Barth, Mary C. 2005 On the prediction of air and pollutant exchange rates in street canyons of different aspect ratios using large-eddy simulation. *Atmospheric Environment* **39** (9), 1567–1574.

Marucci, Davide & Carpentieri, Matteo 2019 Effect of local and approaching stratification on flow and dispersion inside and above a bi-dimensional street canyon. *Building and Environment* **156**, 74–88.

Marucci, D., Carpentieri, M. & Hayden, P. 2018 On the simulation of thick non-neutral boundary layers for urban studies in a wind tunnel. *International Journal of Heat and Fluid Flow* **72**, 37–51.

Uehara, Kiyoshi, Murakami, Shuzo, Oikawa, Susumu & Wakamatsu, Shinji 2000 Wind tunnel experiments on how thermal stratification affects flow in and above urban street canyons. *Atmospheric Environment* **34** (10), 1553–1562.

Wood, C. R., Lacser, A., Barlow, J. F., Padhra, A., Belcher, S. E., Nemitz, E., Helfter, C., Famulari, D. & Grimmond, C. S B 2010 Turbulent Flow at 190 m Height Above London During 2006-2008: A Climatology and the Applicability of Similarity Theory. *Boundary-Layer Meteorology* **137** (1), 77–96.